NUMERICAL SIMULATION OF THE AERATION PATTERN IN THE ATTACHED GROWTH PROCESS WITH DIFFERENT ARRANGEMENT OF BIO-CARRIER

Gasim Hayder[1,*],Puniyarasen Perumulselum[1,*]

[1]*Department of Civil Engineering, Universiti Tenaga Nasional, Malaysia*

[*]For correspondence; Tel. + (60) 89212020, E-mail: gasim@uniten.edu.my

[*]For correspondence; Tel. + (60) 108891589, E-mail: arasan_117@hotmail.com

ABSTRACT: *Aeration is one of the important criteria needs to be considered in order to have a better wastewater treatment system because microorganisms are depending on oxygen to survive and multiply. Wastewater treatment with well-designed aeration system has a direct impact on the performance of the treatment In order to benefit the engineering design of an attached growth reactor, CFD software, ANSYS CFX was used to study the effect of aeration pattern on the behavior of an attached growth reactor. From the CFD analysis, the effect of aeration on the bio-carriers has been studied in term of force exerting on the bio-carriers and air volume fraction results. It can be concluded that, when the distance between the bio-carriers increases, the air circulation is getting better. Better air circulation promotes the good mixing of air with water. With better aeration system, more oxygen can be provided for the multiplication of microorganisms. This will enhance the performance of wastewater treatment system.*

Keywords: aeration pattern, attached growth process, CFD, arrangement

1. INTRODUCTION

Aeration is one of the important criteria needs to be considered in order to have a better wastewater treatment system because microorganisms are depending on oxygen to survive and multiply. Wastewater treatment with well-designed aeration system has a direct impact on the performance of the treatment. Sufficient oxygen need to be supplied to the reactor by the diffusers which provide mixing as well. This action will enhance the ability of microorganisms to oxidize and decompose organic matter [1]. Usage of simulation tool in wastewater treatment system is getting famous. Computational fluid dynamics (CFD) is the simulation tool widely being used in wastewater treatment system. CFD is used to study the fluid flow, heat transfer and other related physical processes in a system. With specific boundary conditions, CFD solves the equations of fluid flow in a interested region. Many researchers are using the CFD technique to study the behavior of the wastewater treatment reactor. Zhuang L. et.al studied the effect of inlet manifold on the performance of a hollow fiber membrane module using CFD simulation. The focused the effect of manifold on the energy consumption and flow distribution for the module. They found that when the area of inlet increases, the energy consumed by the manifold decreases and the inlet holes must be evenly distributed in order to have uniform flow distribution [1]. Besides that, Cahyadi A. et.al studied the membrane fouling in anaerobic fluidized bed membrane bioreactor (AnFMBR) using CFD. They validated a two-fluid model (TFM) against experimental results and used to obtain a comprehensive landscape of local water and particle velocities and concentrations throughout the reactor [2]. Flow pattern analysis and velocity distribution is very important parameters in increasing the treatment efficiency of aeration system. It can be studied using CFD technique. Hadad H. and Ghaderi J. studied the flow pattern in the aeration tank by the activated sludge process using CFD [3]. Similarly, effect of aeration patterns on the flow field in wastewater aeration tanks were studied using CFD by Gresch M. et.al. They adopted different spatial distribution of air diffusers to study the flow field in aeration tank [4]. Moreover, CFD will help researchers to understand the hydrodynamic and mass transfer of a wastewater treatment process. Turbulence effects on hydrodynamics and mass transfer in a packed bed airlift internal loop reactor was studied by Moraveji M. K. et.al. They concluded packing increases the turbulence by 20 % and gas hold-up by 49 %. These parameters will increase the mass transfer more than 43 % [5]. In similar fashion, in this paper, aeration pattern were studied with different arrangement of bio-carrier. This paper aims to study the effect of aeration pattern on the behavior of an attached growth reactor using CFD simulation. In order to benefit the engineering design of an attached growth reactor, CFD software, ANSYS CFX was used to make a simulation and visualize the flow pattern. This simulation is to understand the biofilm growth. Three different distances in between bio-carriers were adopted in this study.

2. METHODOLOGY

2.1 REACTOR SETUP

For the simulation purpose, an aeration tank with volume of 0.8 m3 was created with solid computer-aided design (CAD) software, SOLIDWORKS. The tank has the dimensions of 0.5 m (wide) x 1.6 m (length) x 1 m (height). The tank was created together with total of 33 diffusers inside the tank. The diffuser has 80 mm of diameter.

2.2 BIO-CARRIER

For the simulation purpose, a novel bio-carrier was created using SOLIDWORKS. The bio-carrier was developed with four components attach together. It has two ellipsoids and two straps of voids. The carrier has bigger surface are exposed to water which will increase the growth of biofilm on the surface. Voids have been created to allow the water to flow inside the carrier.

2.3 ARRANGEMENT OF BIO-CARRIER

3 x 3 x 3 arrangement was adopted instead of a single ball to analyze the effect of bulk arrangement on aeration pattern. Three different distances in between 3 x 3 x 3 arrangement of bio-carriers were used to analyze the aeration pattern around the arrangement. 0 mm, 35 mm and 70 mm distances were

used to study how the space in between bio-carriers affects the aeration pattern. Geometry arrangement of a 3 x 3x 3 bio-carriers was chosen because a plane can be created that cuts the center of the tank to analyze the aeration pattern around the center of the bio-carriers

2.4 ANSYS CFX SETUP

ANSYS CFX were used to perform CFD simulation and performed as an Euler-Euler multiphase flow. For discretization of the Reynolds-Averaged Navier-Stokes equations, ANSYS CFX uses a finite volume method. The two phases were involved in this simulation. The phases are water and air. Water was defined as the continuous phase and air as the dispersed phase with 3 mm bubble diameter. Turbulence of the continuous phase is modeled by the SST k-ω model [6]. Default values were used for all the model constants. Dispersed phase and continuous phase were specified to have equal turbulent viscosity. Sato and Sekoguchi model was used for bubble induces turbulanece [7]. Normally, drag force and buoyancy force will be dominant in bubble column-type flows [8]. Both the forces were considered in this simulation too as the system also has bubble column-type flow. Ishii and Zuber model was used to model the drag force. This modal will considers the bubble deformation towards an ellipsoidal shape [9]. Walls and bio-carriers are treated as no-slip boundaries. The air flow was defined as flowing from bottom to top of the tank and the water was in stagnant condition. At the inlet boundary, the total air velocity is 1 m/s. This will result in 0.03 m/s of air velocity for each of the total 33 diffusers. The outlet boundary is modeled as a degassing boundary condition. This condition only will allow air phase to exit the fluid domain. Continuous phase will consider this boundary as a wall and it won't exit the domain. For initial condition, the tank was specified as contain only water with no movement in any direction. Diffusers were neglected in this model since it's not present in the domain physically. The diffusers were imprinted inside the tank. A time step of 0.1 s is used and the simulation captures a period of 2.5 s.

3. RESULTS AND DISCUSSION

Forces acting on the surface and inside the bio-carriers were obtained from ANSYS CFX Post-CFD. Only 9 bio-carriers were chosen for the force analysis because identical bio-carriers in term of its position were ignored. The 9 chosen balls are shown in figure 1. Besides that, the air volume fraction contours also were obtained from x-y plane of the geometry.

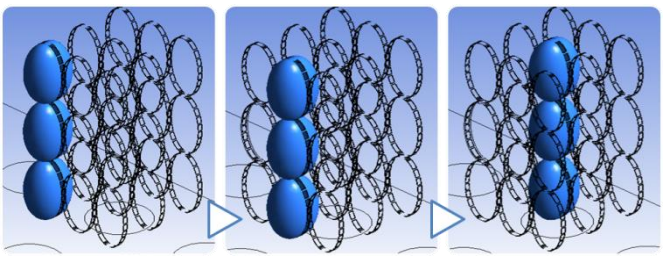

a b c

Fig (1) Bio-Carrier A, B and C (a), Bio-Carriers D, E and F (b) and Bio Carriers G, H and I (c) (From Top to Bottom)

3.1 FORCE ACTING ON THE CARRIERS

The two main forces acting on the bio-carriers are pressure force and viscous force. The obtained values were in Newton units. The pressure force was created by air pressure and the viscous force was generated by viscosity of fluid occupied the domain which is water. The bio-carriers were categorized as corner row carriers (A, B and C), outer middle row carriers (D, E and F) and center row carriers (G, H and I). 3-D cone graphs were created based on the forces obtained from ANSYS CFX post-CFD.

Figure 2 shows the 3-D cone graph of force acting on the corner row carriers. For the close arrangement, carrier C (2.54 N) has the highest force acting on the surface followed by B (1.38 N) and C (1.04 N). In contrast, carrier A (1.53 N) has recorded the highest force in 35 mm distance arrangement flowed by carrier C (1.54 N) and B (1.30 N) while in 70 mm arrangement carrier B (2.84 N) has the highest force followed by carrier and C (1.96 N) and A (1.84 N). Inside the corner carriers, carrier B (0.63 N) recorded the highest force while carrier A (0.30 N) recorded the lowest force in the close arrangement. 0.82 N of force was exerted inside the carrier C for the close arrangement. For 35 mm arrangement, the force acting on the carrier C (0.96 N) were recorded the highest reading while carrier A (0.82 N) recorded second highest reading followed by carrier B (0.58 N). The force acting descends from carrier C (0.91 N) followed by carrier A (0.73 N) and finally carrier B (0.59 N) for 70 mm arrangement.

Figure 3 shows the 3-D cone graph of force acting on the outer middle row carriers. For the close arrangement, carrier F (1.84 N) has the highest force acting on the surface followed by E (1.26 N) and F (0.97 N). In contrast, carrier F (1.19 N) has recorded the highest force in 35 mm distance arrangement flowed by carrier D (0.87 N) and E (0.81 N). Force acting on the surface of the carrier D and carrier E is almost same. In 70 mm arrangement carrier E (1.25 N) has the highest force followed by carrier D (1.17 N) and carrier F (1.08 N). Inside the outer middle row carriers, carrier E (0.96 N) recorded the highest force while carrier D (0.77 N) recorded the lowest force in the close arrangement. 0.47 N of force was exerted inside the carrier F for the close arrangement. For 35 mm arrangement, the force acting on the carrier C (0.63 N) were recorded the highest reading while carrier D and E recorded the same reading which is 0.61 N. The force acting descends from carrier E (0.81 N) followed by carrier F (0.77 N) and finally carrier D (0.59 N) for 70 mm arrangement.

Figure 4 shows the 3-D cone graph of force acting on the center row carriers. For the close arrangement, carrier I (2.66 N) has the highest force acting on the surface followed by H (0.99 N) and G (0.66 N). Carrier I (2.09 N) has recorded the highest force in 35 mm distance arrangement flowed by carrier G (1.07 N) and H (1.02 N). Force acting on the surface of the carrier G and carrier H is almost same. In 70 mm arrangement carrier H (1.82 N) has the highest force followed by carrier G (1.46 N) and carrier I (1.46 N). Inside the center row carriers, carrier G (1.36 N) recorded the highest force while carrier H (1.32 N) recorded the lowest force in the close arrangement. 1.21 N of force was exerted inside the carrier I for the close arrangement. For 35 mm

arrangement, the force acting on the carrier G (1.21 N) were recorded the highest reading while carrier H recorded 0.62 N followed by E (0.50 N). The force acting descends from carrier G (0.80 N) followed by carrier I (0.58 N) and finally carrier H (0.54 N) for 70 mm arrangement.

The forces acting on the carriers are not following any trend because of its position. Some carriers are right above the diffusers while some sharing the air pressure from two diffusers. In the case of the sharing, the distances of the two diffusers from the carries are affecting the forces acting on the carrier. When the diffuser is close to the carrier, it's creating more force on the ball compare to the diffuser far from the carrier. Besides that, viscosity of the fluid is also exerting some forces on the carriers.

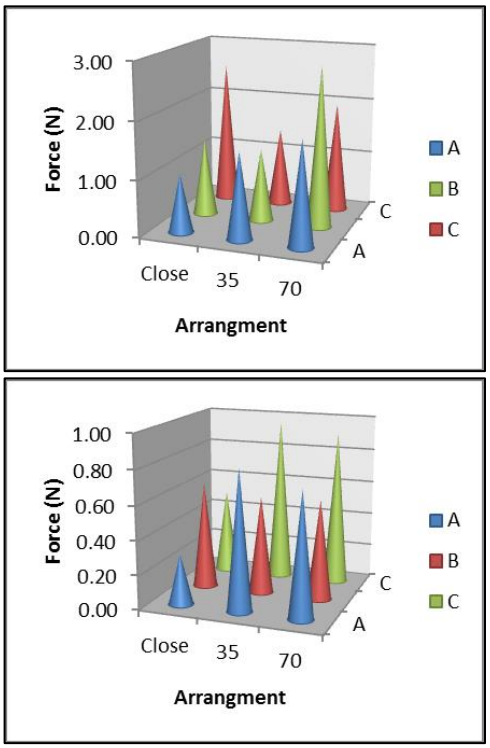

Fig (2) Force Acting on the Surface (Top) and Inside (Bottom) of Corner Row Carriers

3.2 Air Volume Fraction

Volume fraction is defined as the volume of a specific fluid divided by the volume of total fluid in a domain. Air volume fraction results shows the volume of air covered the domain in 2.5 s. Figure 5, 6 and 7 shows the air volume fraction contour for close, 35 mm and 70 mm arrangement respectively. The dead zones of the bio-carriers can be identified by looking at the areas where there are in blue contours which signifies minimum air volume fraction as this indicates the volume of air is very less and results in a poor bacterial growth along this area. As the distance between carrier increases, the time taken for the air to mix with water is decreasing. This has been proven in the figures below as the dead zones are decreasing as the distance between bio-carrier increases. When comparing the outer and center plane carriers, the dead zones are more at center plane carriers in close arrangement and 35 mm arrangement while more dead zones at outer plane carriers in 70 mm arrangement. This is because the planes which are directly beneath of diffusers will receive more air supplies from many diffusers compare to the planes which are not.

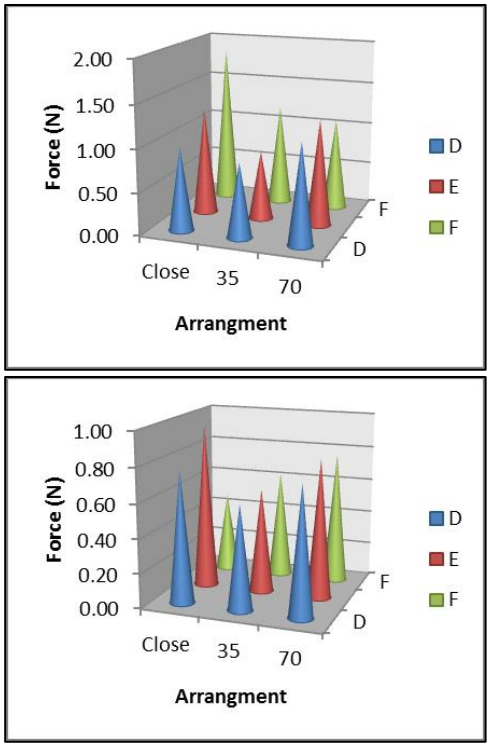

Fig (3) Force Acting on the Surface (Top) and Inside (Bottom) of Outer Middle Row Carriers

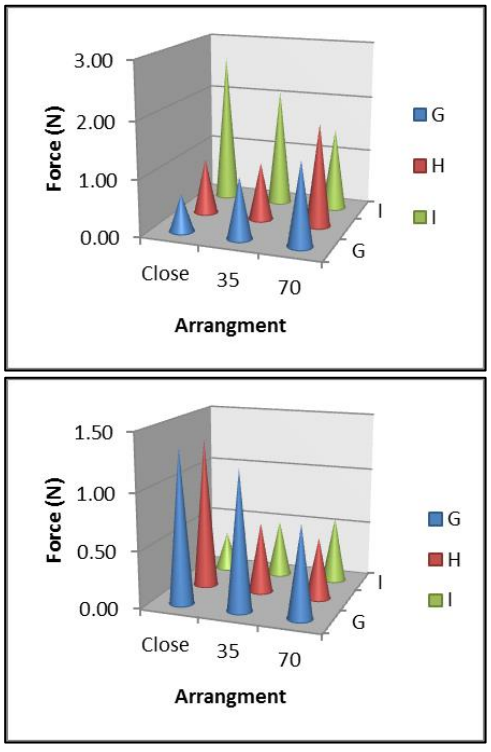

Fig (4) Force Acting on the Surface (Top) and Inside (Bottom) of Center Row Carriers

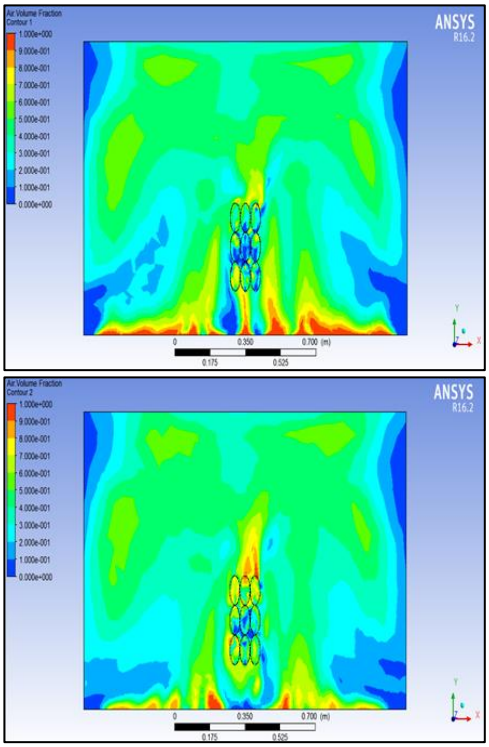

Fig (5) Air Volume Fraction Contour on Center Plane Carriers (Top) and Outer Plane Carriers (Bottom) of Close Arrangement

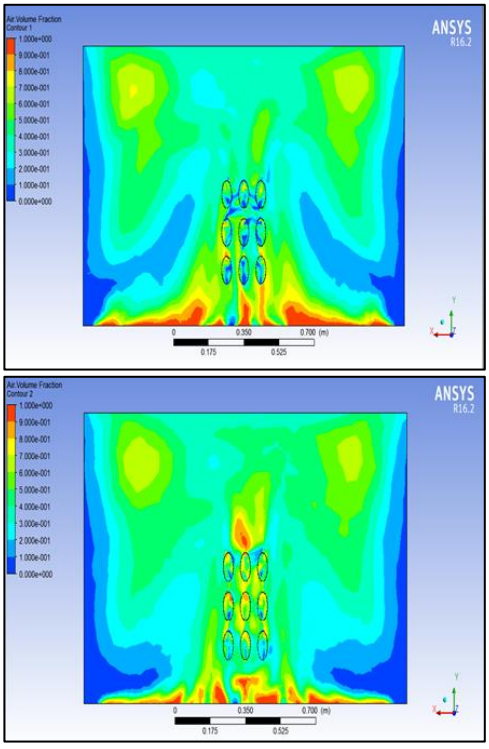

Fig (6) Air Volume Fraction Contour on Center Plane Carriers (Top) and Outer Plane Carriers (Bottom) of 35 mm Arrangement

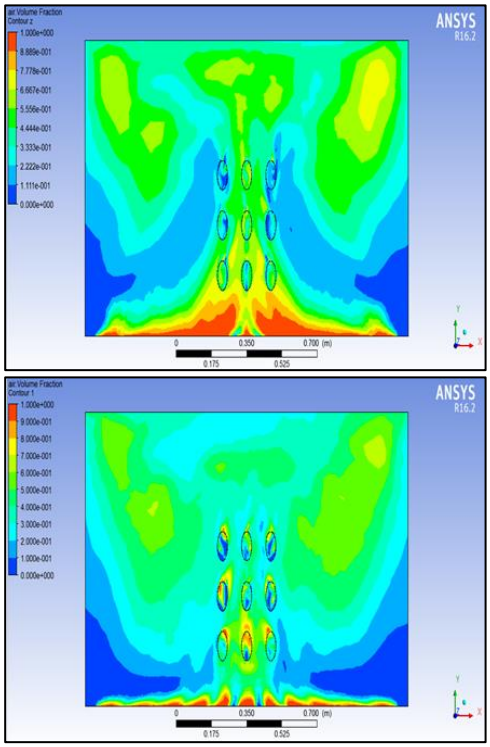

Fig (7) Air Volume Fraction Contour on Center Plane Carriers (Top) and Outer Plane Carriers (Bottom) of 70 mm Arrangement

4. CONCLUSION

CFD has been successfully applied on the three different arrangements of bio-carriers. The arrangements are close arrangement, 35 mm arrangement and 70 mm arrangement. The arrangements of bio-carriers were validated by the force acting on the bio-carriers and air volume fraction at 2.5 s of running time. Aeration pattern determines the flow field in aeration tank because aeration is the main driving force. From the CFD analysis, the effect of aeration on the bio-carriers has been studied in term of force exerting on the bio-carriers and air volume fraction results. Clogging is the major problem in the attach growth process. Clogging occurs because of uncontrolled growth of biofilm. Sloughing is the method to solve the clogging problem. Sloughing is removing the dead layer of biofilm from the surface and inside of bio-carrier. Force exerting on the carrier will promotes sloughing. The force acting on the carrier was obtained from the CFD analysis. These results will help to understand the effect of aeration on sloughing. From the results and discussion part, it can be concluded that, when the distance between the bio-carriers increases, the air circulation is getting better. Better air circulation promotes the good mixing of air with water. Microorganisms in wastewater need oxygen to degrade the pollutants into simple matters. With better aeration system, more oxygen can be provided for the multiplication of microorganisms. This will enhance the performance of wastewater treatment system.

5. ACKNOWLEDGEMENT

The author would like to acknowledge the Ministry of Higher Education of Malaysia for the financial support under Fundamental Research Grant Scheme (FRGS).

6. REFERENCE

[1] Hayder, G., Sidek, L., Mohiyadeen, H. A., Basri, H., Mohd Noh, N., Ahmad, F., and Hock, L. C. "Water Quality Index Score of Different Biomedia for River Water Treatment". 13th International Conference on Urban Drainage, Sarawak, Malaysia, 7-12 September 2014.

[2] Zhuang, L., Guo, H., Dai, G. and Xu, Z.L. "Effect of the inlet manifold on the performance of a hollow fiber membrane module-A CFD study". Journal of Membrane Science, 526, pp.73-93 (2017).

[3] Cahyadi, A., Yang, S. and Chew, J.W. "CFD study on the hydrodynamics of fluidized granular activated carbon in AnFMBR applications". Separation and Purification Technology (2017).

[4] Hadad, H. and Ghaderi, J. "Numerical Simulation of the Flow Pattern in the Aeration Tank of Sewage Treatment System by the Activated Sludge Process Using Fluent Program". In Biological Forum (Vol. 7, No. 1, p. 382). Research Trend (2015).

[5] Gresch, M., Armbruster, M., Braun, D. and Gujer, W. "Effects of aeration patterns on the flow field in wastewater aeration tanks". Water research, 45(2), pp.810-818 (2011).

[6] Moraveji, M.K., Sajjadi, B., Jafarkhani, M. and Davarnejad, R. "Experimental investigation and CFD simulation of turbulence effect on hydrodynamic and mass transfer in a packed bed airlift internal loop reactor". International Communications in Heat and Mass Transfer, 38(4), pp.518-524 (2011).

[7] Menter, F.R. "Two-equation eddy-viscosity turbulence models for engineering applications". AIAA journal, 32(8), pp.1598-1605 (1994).

[8] Sato, Y. and Sekoguchi, K. "Liquid velocity distribution in two-phase bubble flow". International Journal of Multiphase Flow, 2(1), pp.79-95 (1975).

[9] Ishii, M. and Zuber, N. "Drag coefficient and relative velocity in bubbly, droplet or particulate flows". AIChE Journal, 25(5), pp.843-855 (1979).

*For correspondence; Tel. + (60) 89212020, E-mail: gasim@uniten.edu.my

*For correspondence; Tel. + (60) 108891589, E-mail: arasan_117@hotmail.com